A Dark Matter Simulation of the Galactic Centre Photon Excess in the pMSSM and an Estimation of the Uncertainties

Radboud University Nijmegen
Nijmegen, September 15, 2016

Jonas Würzinger

Under Supervision of:
dr. Sascha Caron - Experimental High Energy Physics
Prof. dr. Ronald Kleiss - Theoretical High Energy Physics

A Thesis submitted for the Degree Bachelor of Science
and for the Radboud Honours Academy

Acknowledgments

I am grateful to my family and especially my parents for their support during all of my study. I want to thank the people of the Honours Programme for making it possible for me to do such interesting research this early on in my career and to take part in the SUSY 2016 conference and travel all the way to Australia.

Also, I am extremely thankful to Peter Skands for his support in organising my journey and for giving me the opportunity to learn from his ideas. I want to thank both of my supervisors for their support and the interesting and challenging tasks they had prepared for me. I want to especially thank Melissa, Bob and Ruud for always having time for me whenever I came running, saying "Sascha wants me to . . . ".

Thank you all!

Contents

Abstract

The Galactic Centre γ-ray excess is simulated in the pMSSM for a neutralino pair with masses of 84.9 GeV annihilating into a pair of W-bosons. The process is simulated by $\gamma\gamma \to W^+W^-$ in `Herwig++ 2.7.1` and by $\nu_e\overline{\nu_e} \to W^+W^-$ in `PYTHIA 8.2.19` and `PYTHIA 6.4.16`, all with standard tunes. The spectrum is also obtained by the 2013 Innsbruck tune in `PYTHIA 6.4.28` and the 2013 Monash tune in `PYTHIA 8.2.19`. These spectra are compared with a spectrum tabulated in `DarkSUSY 5.1.1` as well as the data. These comparisons confirm an astrophysical error of roughly 10% on the spectrum produced by `PYTHIA 8.2.19`, which is needed to fit the data. The electron-, positron-, proton- and anti-proton-spectrum are shown to further test the agreement of the simulations.

1 Introduction

1.1 Dark Matter

Dark matter (DM) is one of the greatest mysteries of physics nowadays. Multiple calculations and observations indicate its existence. It is, for example, possible to calculate the existing mass of the milky way or other galaxies from their rotational spectrum and then compare this with the observable mass, thus the amount of matter which can be seen by light that it emits [1, 2]. One can also measure the gravitational lensing of clusters [3], making use of the fact that every massive object curves spacetime and thus also the path of light. Furthermore, the existence of dark matter can be proven by an analysis of the properties of the cosmic microwave background [4].

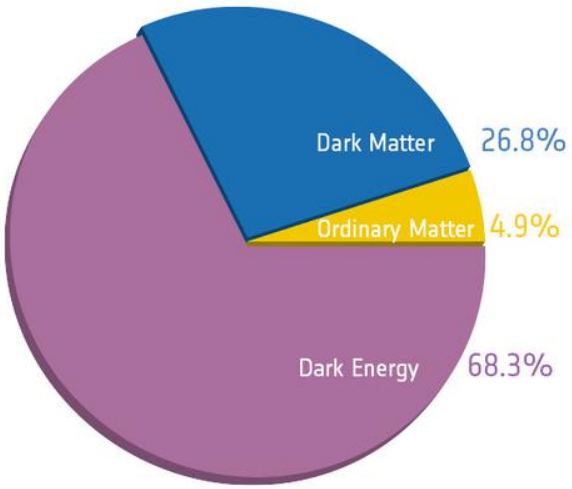

Figure 1: A pie chart of the universe's mass. Source: https://www.ucl.ac.uk/star/research/cosmology/science/images/figures/planck_cosmic_pie.

Dark matter makes up a dominant part of the universe's density, as can be seen in figure 1. However, very little is actually known about it. It is known that it is massive and "dark", which means that it does not radiate electromagnetic waves, i.e. it has no charge and also no colour. From the calculations mentioned above, some details about the spacial distribution can also be concluded.

From the fact that it is "dark", it is possible to conclude that such a particle can neither have a charge nor interact by the strong interaction. Both conclusions can be drawn due to the fact that dark matter has not been observed yet. This includes that particles like neutrinos could in principle be dark matter candidates, however they do not have enough mass to explain the total dark matter mass by themselves, so they need a much heavier right-handed neutrino in order to explain the observations. They are also not ideal as a DM candidate as they would involve hot dark matter, i.e. DM particles moving at a relativistic speed. This is unlikely due to the stable spherical DM distribution in galaxies.

In the standard model there are no particles which can explain the dark matter observations, so the particle that we are looking for can not be a standard model particle. As a DM candidate has to be uncharged and can not have a colour, we know that if a dark matter particle has any standard model interaction, it is the weak interaction. Such a particle is often referred to as a Weakly Interactive Massive Particle (WIMP).

Again, neutrinos for example are also candidates for DM, but WIMPs are widely used because they are able to explain the dark matter density in the milky way by just assuming that the dark matter particle has about a mass of a boson ($\mathcal{O}(100)$ GeV) and interacts via the weak interaction. This is the so-called "WIMP miracle". Also, WIMPs involve a cold dark matter explanation, so they agree with the spherical DM distribution.

But knowing this is not enough for a complete description of a possible dark matter particle. Thus the search for a direct or indirect detection of dark matter is an important challenge in physics, as well as finding a suitable model. The underlying theory of this thesis will be discussed in section 1.2, and section 2 in more detail.

1.2 Supersymmetry

The theory of Supersymmetry (SUSY) exists for various reasons and only one of these is the description of a possible DM particle. SUSY provides a description of other dark matter candidates than a WIMP as well, but WIMPs are the most widely used particles because of the WIMP miracle.

But in every case, a theory, which introduces new particles, is needed. SUSY does that by stating that every fermion (half-integer spin particle) has a corresponding boson (integer spin particle) with otherwise the exact same attributes, as pictured in figure 2. This means that there are a lot of candidates for dark matter. However, it is assumed that SUSY particles have higher masses than standard model particles, as, again, no such particles have been found yet. A broken symmetry might seem undesirable, but the standard model also involves symmetry breaking (Higgs mechanism). Furthermore, there are other, theoretical reasons for Supersymmetry to exist, which will not be named here. It is untrivial to formulate a theory within SUSY that satisfies all theoretical restrictions. At this point, we only know which theoretic framework to use, the details of the theory will be discussed in section 2.

Independent of these details, it is important that the theory can be tested. Hence we need data which indicates the existence of DM, on which we can test the theory and which helps us develop a more detailed model. A particular example of this data will be discussed in the next section.

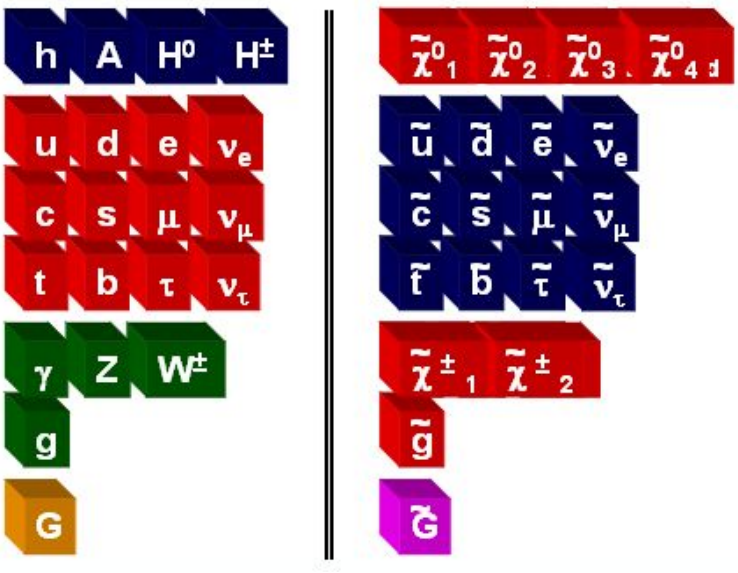

Figure 2: The supersymmetric model. Source: http://www.pd.infn.it/~dorigo/susyspectrum.jpg.

1.3 The Fermi GeV excess

The Fermi/LAT satellite found an excess of γ-rays in the region of the galactic centre of the milky way, which still remained after subtracting the known astrophysical sources like particles radiated due to the cosmic rays travelling through the interstellar medium [5, 6][1]. At this region, the expected DM density is very high, so it is reasonable to assume that these γ-rays are produced by dark matter. It is known from clustering simulations that the dark matter distribution extends beyond the galactic plane in a halo centred around the galactic centre [7]. As the signal, just like the expected dark matter density, extends well beyond the plane of the milky way ($\geq 10°$), it is likely to be caused by dark matter [8].

However, there are different explanations for the excess. The galactic centre is an extremely bright region, meaning that the identification of (point)sources and therefore also the subtraction of the known background are both equally difficult. Theories involving astrophysical sources are also possible. One other possible explanation for the galactic centre excess, besides dark matter, are Millisecond Pulsars and Young Pulsars. Astrophysicists first developed a model involving Millisecond pulsars[2] [9], but those would involve an additionally large component of radiation in the radio-regime, which has been found to be less then expected. Therefore a new model was developed, in which the population of pulsars is split up in Young Pulsars, which do not radiate the missing component [10], and Millisecond Pulsars, which still radiate in the radio-regime. The extension of the signal beyond the galactic plane can be used as an argument against this model, however this is not enough to exclude it.

A direct comparison of the two theories might make it possible to draw conclusions about their validity. Such a comparison is shown in figure 3. The DM model used is not the same as in this thesis, but the plot is only shown to compare the theories in general. This comparison reveals that the solutions are too similar to exclude one or the other. The solid black lines in figure 3 show the uncertainty of the measurement. Both of the possible solutions fit similarly well. The problem in this case is the large uncertainty on the measurement due to the difficult subtraction of the known background. Also, there are various different models on both sides which try to explain the excess which in general leaves room for variations on both fits as well. Therefore, an exclusion of one of the explanations is extremely difficult. This makes it especially important to handle the model uncertainties with care.

[1] These articles are only examples of work that has been done to subtract the background noise and other sources that cause the signal to deviate.

[2] In this model the radiation would be produced by charged particles moving through the magnetic field of the pulsars.

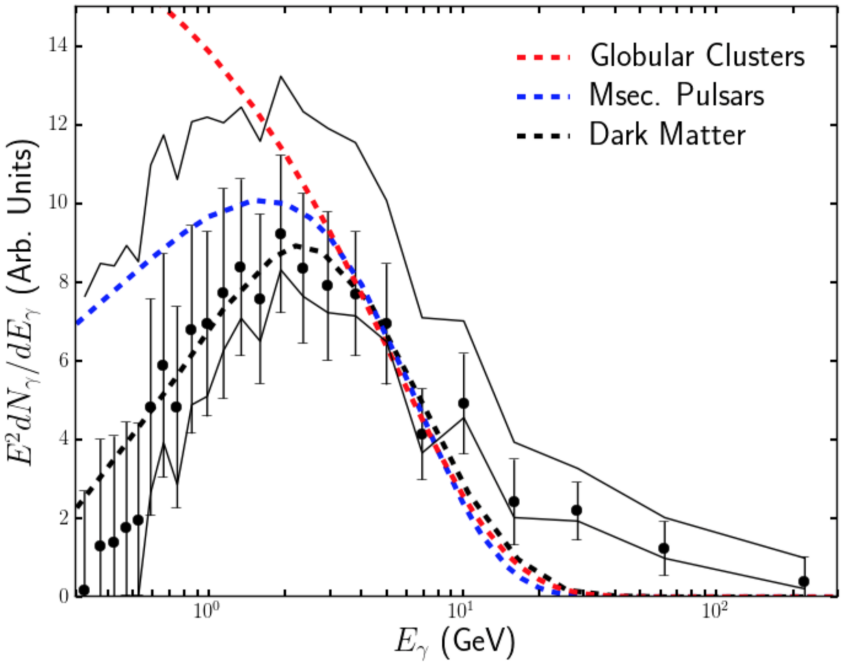

Figure 3: The different predictions for the GC access, with the measurement (black solid). Here the DM solution is an annihilation into $b\bar{b}$. Credit: [9]

2 The Dark Matter Model

As mentioned before, we consider the dark matter particle to be a WIMP and Supersymmetry is useful to describe such particles. Even if a dark matter particle has not been found yet, there are observations that lay restrictions on DM candidates. This limits the parameters used in SUSY models. The number of parameters involved is generally still very large. Usage of the Minimal Supersymmetric model (MSSM) already limits the number of parameters of the model. If one then uses phenomenological constraints, the number of parameters reduces from 105 to 22 (pMSSM), but this number can still be reduced by other calculations. In the end, there are 19 parameters remaining [11].

Most of them are masses of the supersymmetric particles and a large part of them is not relevant for this case. As a matter of fact, finding a solution in this 19-dimantional parameter space is not straightforward, because most of the parameters are connected in a very complex way, while restrictions like obtaining the correct Higgs mass or the correct mass of the Z boson still have to be satisfied. This is the reason why there are many different SUSY theories predicting different masses for the particles. These are then - unsuccessfully until now - searched for in colliders like the LHC. In this model, the lightest neutral SUSY particle (neutralino) is the Dark Matter candidate with a mass of 84.9 GeV. The production of photons by dark matter in general is described in [12].

There are three different types of solutions for the Galactic centre excess itself. The first solution involves a bino-higgsino neutralino pair ($\sim$ 50% bino and 50% higgsino) with masses between 84 - 92 GeV to annihilate into a W^+W^- pair. The second one would be a bino-wino-higgsino neutralino pair ($\sim$ 90% bino, 6% wino and 4% higgsino) with masses between 87 - 97 GeV which can also annihilate into W^+W^-. The third solution involves annihilation of a mostly ($\sim$ 99%) bino neutralino pair with a mass range of 174 - 187 GeV into a pair of top quarks. The bino is the superpartner of the $U(1)$ gauge field, the wino the superpartner of the W boson and the higgsino the superpartner of the

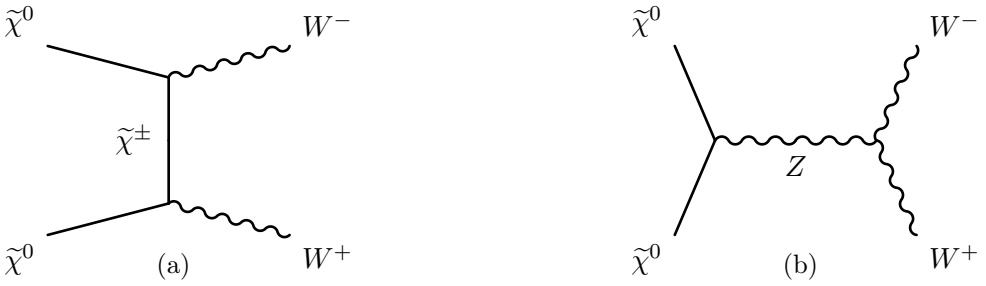

Figure 4: The dominant annihilation diagrams for the Wino/Higgsino component of the neutralino $\widetilde{\chi}_0^0$ into a pair of W bosons.

Higgs boson. These neutralino states are not actually the mass eigenstates, but linear combinations of them are. This is called neutralino mixing. The parameters of these linear combinations, i.e. the percentages, are variable.

Both solutions that produce a pair of W bosons annihilate following the diagrams shown in figure 4. Both diagrams are only possible for the wino and the higgsino component and not for the bino component as it can neither couple to itself nor to a chargino $\widetilde{\chi}^\pm$. Here, the dark matter relic density used is $0.06 < \Omega h^2 < 0.13$ [11]. The dark matter relic density is the density of dark matter that is still left after the hot early phase of the universe, where a transition between DM and regular matter was easier as the thermal energy of the particles was much higher.

The W^+W^- pairs could, in the end, produce photons by their decay into quarks, which in turn radiate gluons. These produce more quarks and they then can decay into colourless hadrons. These hadrons (mostly π^0) radiate photons, but they are produced by other steps in the chain as well [11]. These photons are then measured by Fermi/LAT. In simulations, the production of photons is largely dependent on the fragmentation function, which describes the fragmentation of partons, but also on other things like the hadronisation (the way new hadrons are formed from quarks and gluons). So different models for these diagrams produce different photon spectra.

If all the details of the model are known, it is possible to predict the photon spectrum produced by such particles. Explanation follows in the next section.

2.1 The Simulation

Figure 5: The two dominant annihilation diagrams for $\nu_e\overline{\nu_e} \to W^+W^-$.

It is possible to simulate the photon spectrum of the annihilation of neutralinos using Monte Carlo simulations like `PYTHIA` [13]. One such simulation is pictured in figure 6. In this figure, the excess was simulated using an annihilation of (anti-)neutrinos with a kinetic energy of 84.9 GeV into a pair of W bosons instead of neutralinos with a mass of 84.9 GeV annihilating into a pair of W bosons. The two most relevant diagrams for the annihilation of these neutrino-anti-neutrino pairs are pictured in figure 5. When compared with figure 4 the similarities between these two diagrams are relatively clear. A more detailed discussion of them can be found in section 4.6.

The main error made by this approach lies in the normalisation of the spectrum. The normalisation of the measured spectrum depends strongly on the dark matter density in the galactic centre and the cross section of the decay, which are both only known with rather large errors. Thus the produced spectra have to be normalised in order to enable comparisons with the data as only the shapes of the spectra are relevant in this study.

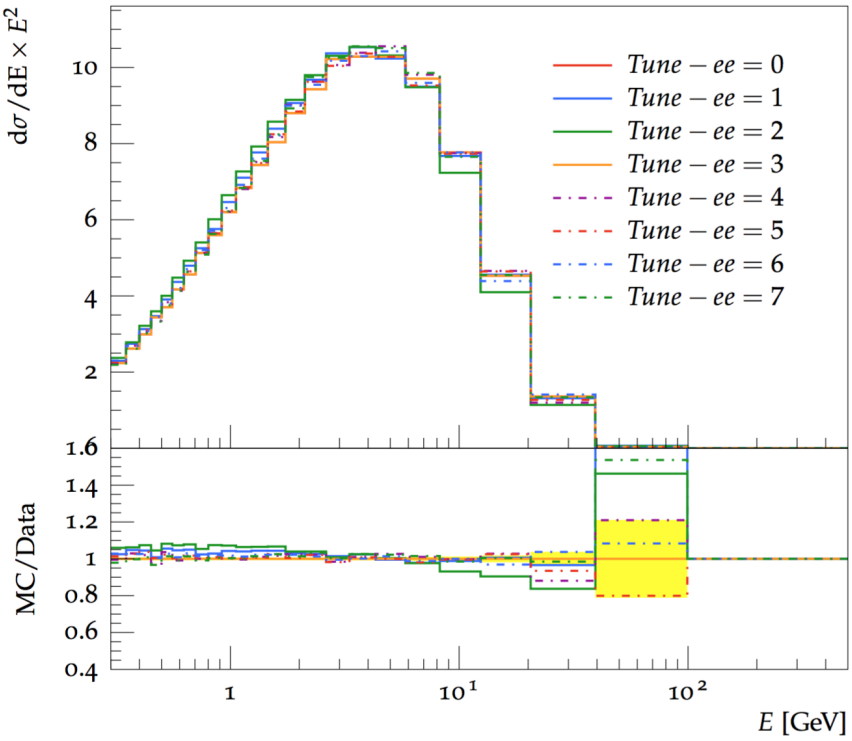

Figure 6: Simulation of the photonspectrum for $\nu_e\overline{\nu_e} \to W^+W^-$ with neutrino energies of 84.9 GeV in `PYTHIA 8`. Credit: [11].

The tunes in figure 6 refer to the different sets of parameters which were obtained by different approaches by optimising the performance of `PYTHIA 8` with respect to data obtained by e^+e^- collisions like in LEP. In figure 6 it also can be seen that the simulated spectrum deviates by roughly 10% from the data. The model used in figure 6 gives a promising result with a p-value of 0.35 if high-energy physics uncertainties are included and 0.03 if they are not included. This number is largely dependent on the tune. So, there has to be an additional 10% error on top of the simulation in order to be able to explain the data. It was stated that this estimated uncertainty is indeed reasonable in order to account for additional physical uncertainties in the model. This fit is much better than the $t\bar{t}$ solution, because this solution only leads to a p-value of 0.1, even if an additional 10% uncertainty is included [11].

3 Proposed Research

In summary, the GC excess can be explained by different types of solutions, like the annihilation of dark matter particles into a pair of W^+W^- or $t\bar{t}$ or by Millisecond or Young pulsars, while they are too similar to draw definite conclusions about the validity of the models. The model in [11] only obtains a good fit, if an additional error is included.

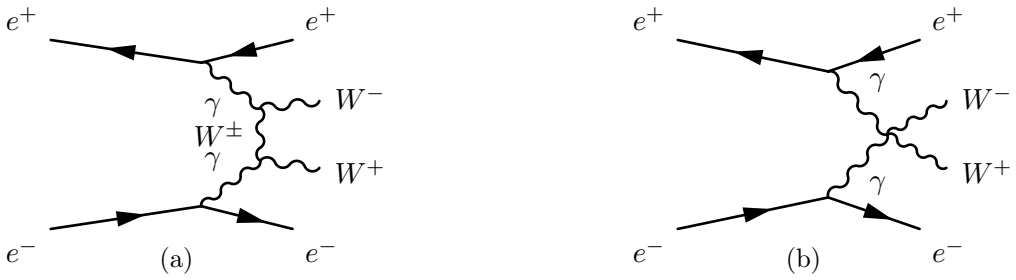

Figure 7: The two dominant annihilation processes for $e^+e^- \to \gamma\gamma \to W^+W^-$.

Thus, it is crucial to this theory to test this estimated uncertainty and maybe give a more detailed or justified estimate. This test will be performed in this thesis.

In order to do so, the simulation mentioned above will first be repeated with `PYTHIA 8`. But as already stated, using different tunes in the same Monte Carlo (MC) generator does not account for any physical systematic errors from the model itself, so it is necessary to also use different MC generators as well. These errors involve uncertainties in for example the fragmentation function, which can not be measured directly, σ_{p_T}, which is the amount of transverse momentum that is allowed in the decay chain, or the hadronisation. In this case these different simulations will be `PYTHIA 6` and `HERWIG++` [13, 14]. Especially `HERWIG++` uses a different model for, most importantly, the fragmentation, which results in a different prediction for the photon spectrum, as mentioned before.

This difference can be used to check the estimate of the physical error on top of the `PYTHIA 8` spectrum of 10% made by the MC generator. In this work, we focus on the W^+W^- solution of [11], because it produces the better fit compared to the $t\bar{t}$ solution with a maximum p-value of 0.35 rather than a maximum of 0.1 for the $t\bar{t}$ solution.

4 Results

In `HERWIG++`, the annihilation of the neutralinos was estimated by an annihilation of photons (figure 7), because the matrix element for an annihilation of neutrinos is not implemented in `HERWIG++`. The process is chosen for reasons named in section 4.6.

Due to the fact that the $e^\pm$ give almost all their energy to the photons, they can easily be filtered out in the end and do not interact with other particles, so there are no unwanted byproducts. The only remaining problem is that the photons then do not have the exact energy of 84.9 GeV, but can rather also have lower energies, as shown in figure 8. This results in an additional uncertainty for the photon-spectrum produced by `HERWIG++`. So, it was chosen to only take events into account where the energy of both incoming photons is at least 99% of the energy of the incoming electrons/positrons. This eliminates this uncertainty nearly completely.

In figure 9, the two spectra produced by `HERWIG++` with and without the filtering are shown. The filtered spectrum, i.e. the spectrum for which both incoming photons need to have at least 99% of the energy of the incoming $e^\pm$, will be used in the following, as it is a much better approximation of the simulation of the dark matter annihilation. The spectra differ the most for higher energies, where the filtered version produces more photons.

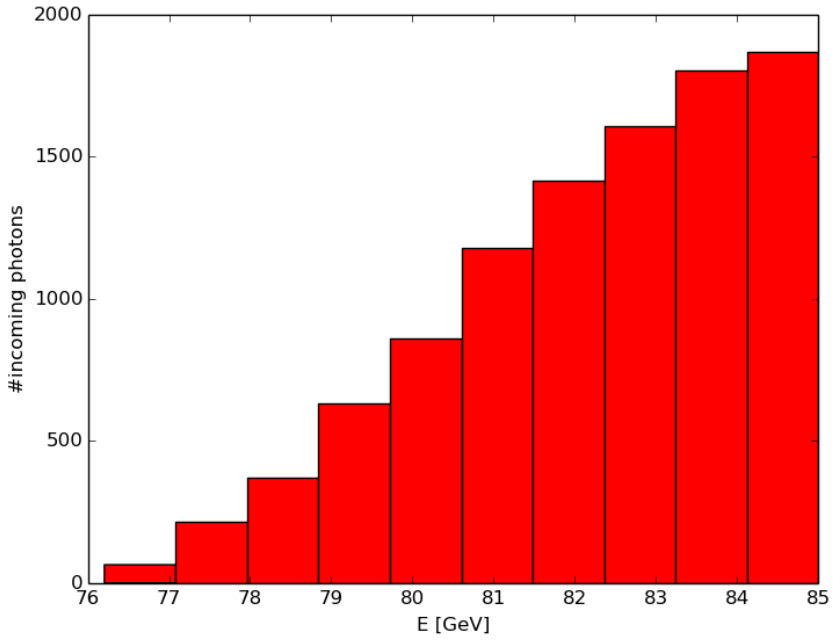

Figure 8: The distribution of the incoming photons for the processes shown in figure 7.

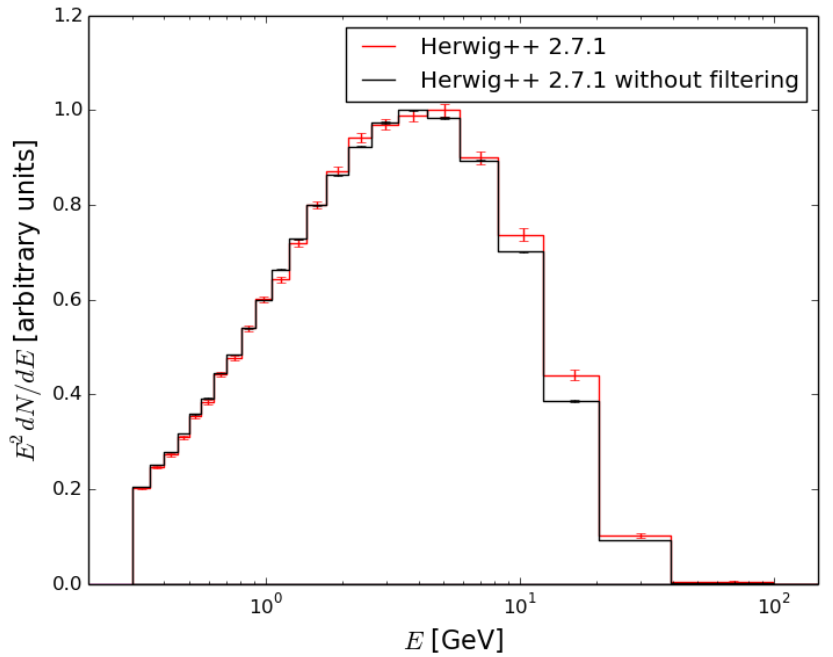

Figure 9: A comparison of the two normalised spectra produced by `HERWIG++` with and without filtering for energy.

4.1 Bremsstrahlung

As HERWIG++ does not include bremsstrahlung as a final state radiation component [15], it is likely that HERWIG++ will drop off at higher energies with respect to other simulations. This is tested by switching off this radiation in PYTHIA 8 and comparing the produced spectra, see figure 10.

In this case, the bremsstrahlung in PYTHIA 8 has been switched off by switching all the flags TimeShower:QEDshowerByQ, TimeShower:QEDshowerByL and TimeShower:QEDshowerByGamma off. Here, the hypothesis of the spectrum produced by HERWIG++ dropping off at higher energies due to a missing bremstsrahlung component in the final state radiation is in agreement with the simulation.

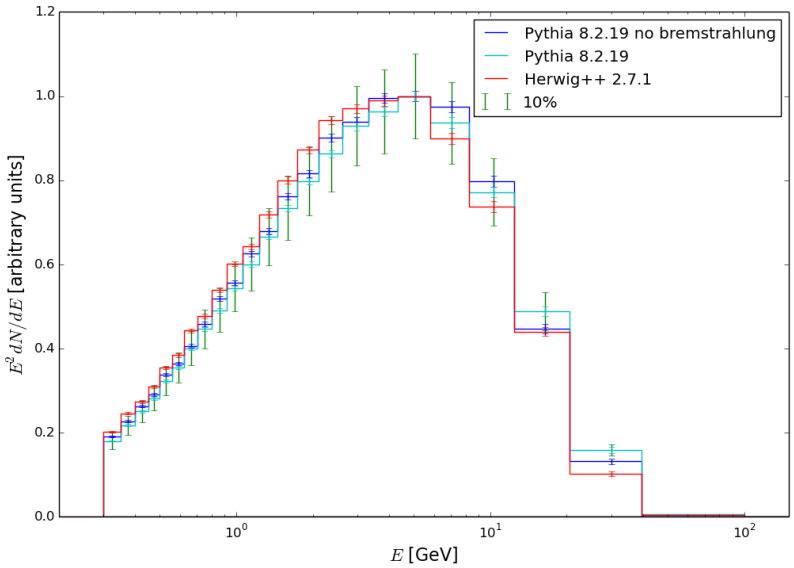

Figure 10: A comparison of the normalised spectra produced by HERWIG++ and PYTHIA 8 with and without bremsstrahlung.

4.2 Standard Tunes

The process used in both PYTHIA 6 and PYTHIA 8 is the same as pictured in figure 5. A comparison of this different approach with the one for HERWIG++ can be found in section 4.6. Figure 11 shows a unnormalised spectrum produced by the three generators, while the default tune was used for all of them. The difference between PYTHIA 6 and PYTHIA 8 might seem large, but it is a direct result of the different default tunes. Also, HERWIG++ produces more photons for energies up to the peak. The spectrum of HERWIG++ decreases relative to PYTHIA for high energies because HERWIG++ does not include bremsstrahlung as a final state radiation component (see section 4.1). This means that HERWIG++ produces more photons in general, but then drops below the PYTHIA spectra due to the missing component. The errors of all spectra are not uncertainties of the simulations themselves, but rather only statistical errors. The reason for this is that it is very difficult to include model uncertainties into the simulation. Also, there is an additional uncertainty involved, as we only approach the neutralino annihilation by other processes.

Here, it can already be seen that the 10% error estimate is fairly good. Most importantly, the peaks of the different spectra are all positioned at $3 \leqslant E\gamma \leqslant 6$ GeV, so they all agree very well with

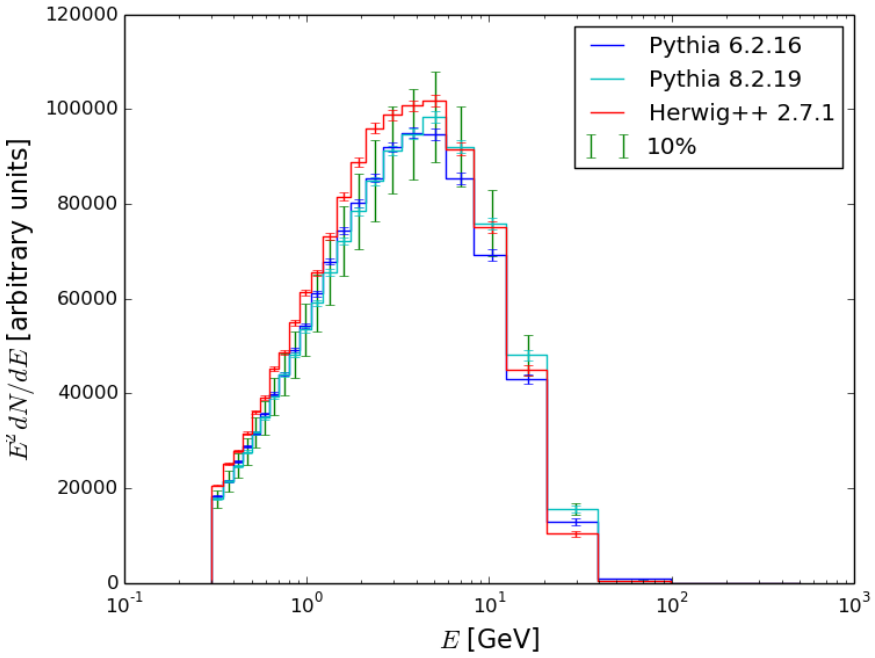

Figure 11: The simulation performed with default tunes. The spectra are not normalised.

the Fermi/LAT observation, which estimates the position of the peak at $1 \leqslant E\gamma \leqslant 5$ GeV [11]. A more detailed comparison with the data will be performed in section 4.5.

As noted earlier, the most relevant are the normalised spectra. At this point we specifically do not choose to normalise by total flux (i.e. by the integral) because in that case, bigger bins have a higher weight and the largest bins are lying at higher energies. These bins are only filled with a low number of particles, meaning that the uncertainty in both number and energy is large. Hence, by normalising by integral, one would assign a higher weight to less well-known quantities. This would influence the normalisation greatly, but it should not.

So instead, it was chosen to normalise the spectra by their peak flux, as shown in figure 12. Here, the spectra are mostly in agreement within the 10% error estimate, except for high energies, which was already partly identified as the missing bremsstrahlung component in `HERWIG++`. The difference between `PYTHIA 6` and `PYTHIA 8` remains for nearly all energies. If this difference is a product of the use of very differently old tunes, it can be reduced by using newer tune for especially `PYTHIA 6` (see section 4.3). This is likely to be the case, as this versions default tune is relatively old.

For a further investigation of the spectra's agreement, their ratios are shown in figure 13. Again, agreement at higher energies is not very important, because the involved uncertainties are so large. Both ratios increase for energies higher than the peak energy of roughly 5 GeV due to `HERWIG++` dropping off at higher energies. So this effect is again a result of `HERWIG++` missing bremsstrahlung, which has been shown in section 4.1. The difference between `PYTHIA 6` and `PYTHIA 8` for lower energies is more than expected, but it can be reduced by switching to newer tunes.

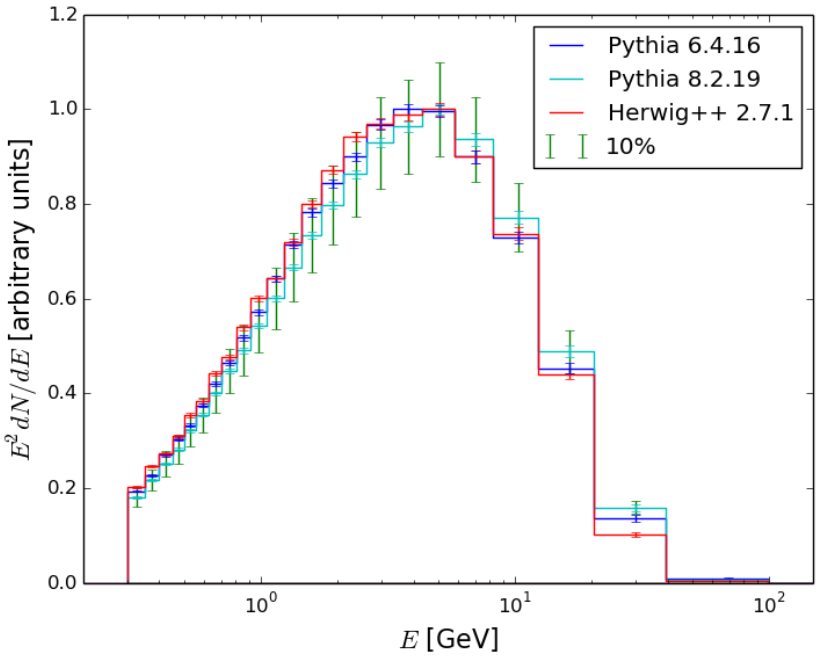

Figure 12: The simulation performed with default tunes. The spectra are normalised.

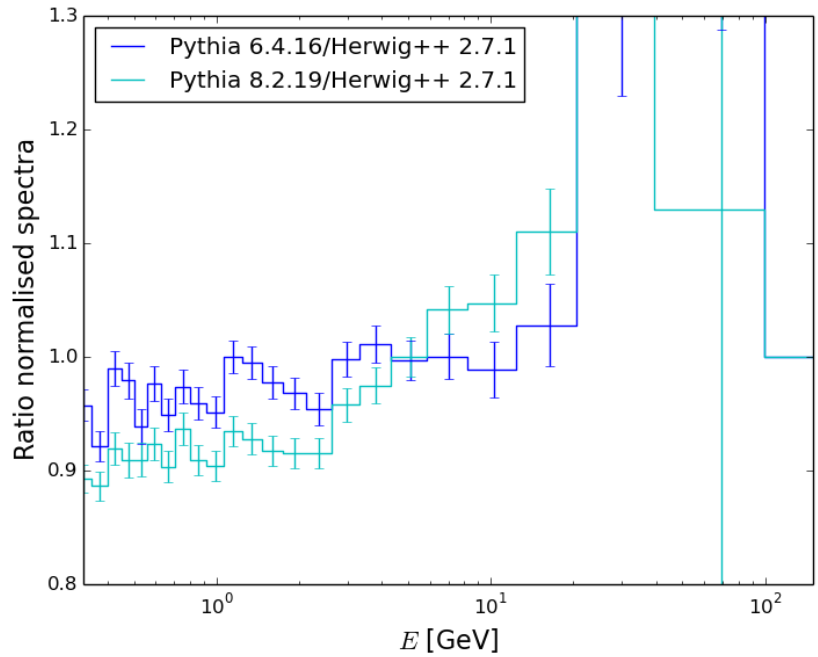

Figure 13: Ratio of the normalised spectra for default tunes.

4.3 Newer Tunes

In order to obtain a more reliable result and also in order to be able to compare PYTHIA 6 and PYTHIA 8 better, the produced spectra are also investigated for newer tunes. In the case of PYTHIA 6 the 2013 Innsbruck tune [16] and in the case of PYTHIA 8 the 2013 Monash tune was used [17]. It is quite important to state that these tunes were developed by different people. So, they are based on different assumptions and approaches such that similarities in the spectra due to similarities in the tunes are less likely. This makes the comparison easier and more reliable. One could argue that the tunes are still correlated because they are both based on the same LEP data, but avoiding this is extremely difficult.

A tuning of HERWIG++ has not been performed here, because there are no tunes for HERWIG++, but rather a variety of switches with which users can perform the tuning themselves. Although this would in theory be possible, we have chosen not to do it at this point, but rather only use different tunes for both versions of PYTHIA, as it goes beyond the scope of this project.

The photon spectrum produced by the different tunes are shown in figure 14. These, again, are not normalised in order to make comparisons between the different MCs easier. The difference

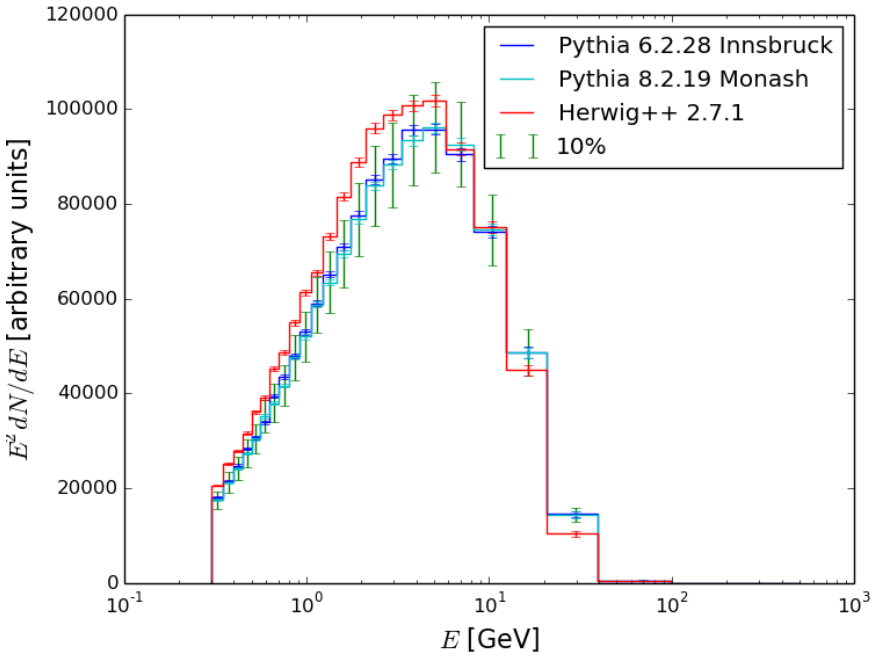

Figure 14: The simulation performed with with the 2013 Innsbruck tune [16] used for PYTHIA 6 and the 2013 Monash tune [17] used for PYTHIA 8. The spectra are not normalised.

between PYTHIA 6 and 8 in figure 14 is a lot smaller after switching tunes, as expected in section 4.2. They now agree very well within the estimated error. The peak in PYTHIA 6 is shifted a little more towards lower energies. A remaining question is why HERWIG++ produces more photons for low energies.

Figure 15 shows the renormalised photon spectra for the newer tunes for both versions of PYTHIA. Here we see a good agreement within the 10% error estimate, apart from very high energies for HERWIG++, where HERWIG++ is most likely the less reliable spectrum. This also can be seen in figure 16, where the ratios of the spectra are pictured. In this plot we also see a much better agreement

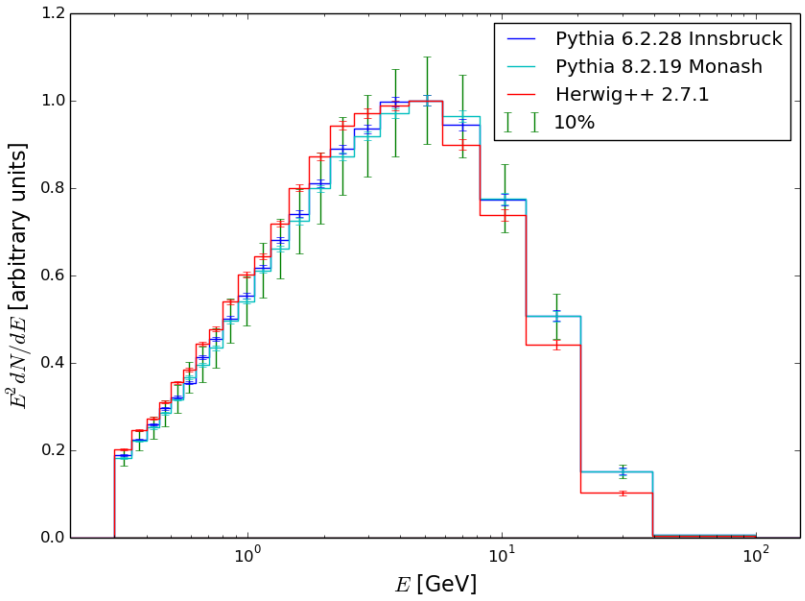

Figure 15: The simulation performed with with the 2013 Innsbruck tune [16] used for `PYTHIA 6` and the 2013 Monash tune [17] used for `PYTHIA 8`. The spectra are normalised.

between the two versions of `PYTHIA` than before.

Again, high energies are not as relevant due to the large uncertainties in both energies and photon counts, as well as `HERWIG++` dropping off, but for energies up to about 10 GeV the spectra indeed agree very well within an error of 10%.

Both versions of `PYTHIA` are still mostly in agreement with `HERWIG++`, as their ratios with `HERWIG++` mostly lie within the 10% band, which is about the same uncertainty as was needed for `PYTHIA 8` to fit the data. As the ratio of `PYTHIA 8` with `HERWIG++` lies within about a 10% band, it can be concluded that `HERWIG++` agrees with the error estimate. The similarity between the two ratios is a further confirmation.

So far, it seems like the estimate of the error was indeed reasonable, so `PYTHIA 8` would fit the data. To confirm this, it is possible to compare the produced spectra to a spectrum obtained from `DarkSUSY` [18]. This can be found in section 4.4. Also, in section 4.5 the simulations will be compared with the data from Fermi/LAT in order to strengthen the conclusion.

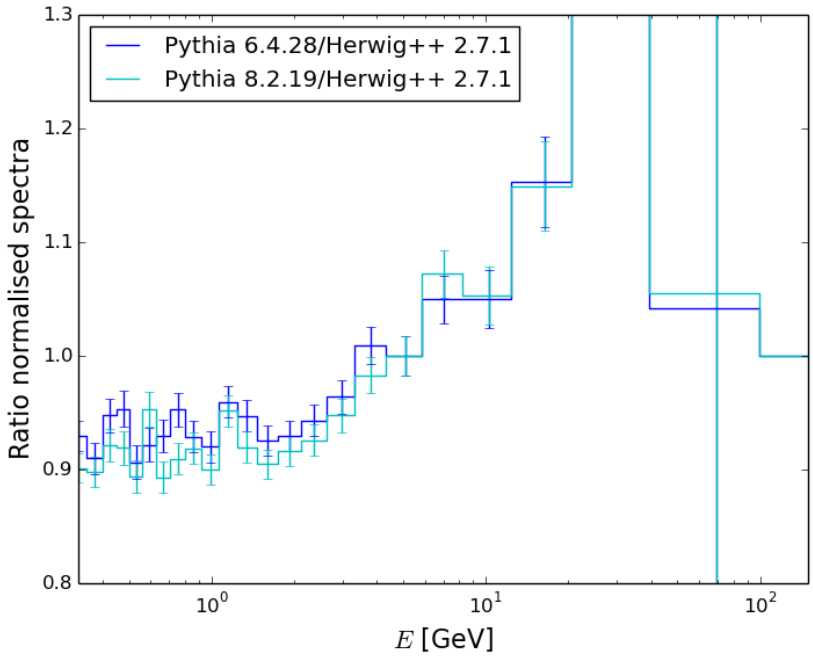

Figure 16: Ratio of the normalised spectra with the 2013 Innsbruck tune [16] used for `PYTHIA 6` and the 2013 Monash tune [17] used for `PYTHIA 8`.

4.4 DarkSusy

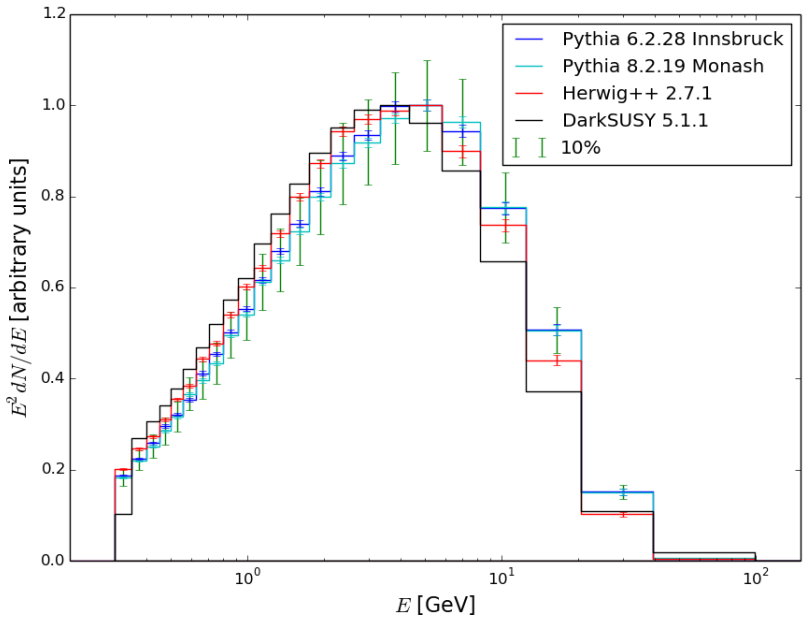

Figure 17: The normalised spectra performed with the newer tunes, including a simulation in `DarkSUSY 5.1.1`.

The normalised photon spectra produced by the 2013 Innsbruck and the 2013 Monash tunes for both versions of PYTHIA and the default tune for HERWIG++ including a spectrum produced by DarkSUSY are pictured in figure 17. This program can be seen as a separate source of such a spectrum and might therefore compare differently to the simulations performed by Standard Model MC's. DarkSUSY has a tabulated spectrum included.

Again, all of the simulations agree quite well. Interestingly, the DarkSUSY spectrum agrees very well with HERWIG++ for higher energies, so where both versions of PYTHIA do not. DarkSUSY also produces more photons than the Standard Model simulations at lower energies, where it again agrees better with HERWIG++. DarkSUSY does not agree with PYTHIA 8 (and 6) within the estimated error, but the peak position of the DarkSUSY spectrum agrees well with all of the other spectra. Still, it has to be kept in mind, that the 10% error is not enough to let DarkSUSY and both versions of PYTHIA agree. This can be confirmed by figure 18. The ratio of DarkSUSY with HERWIG++ lies within 1 ± 0.1

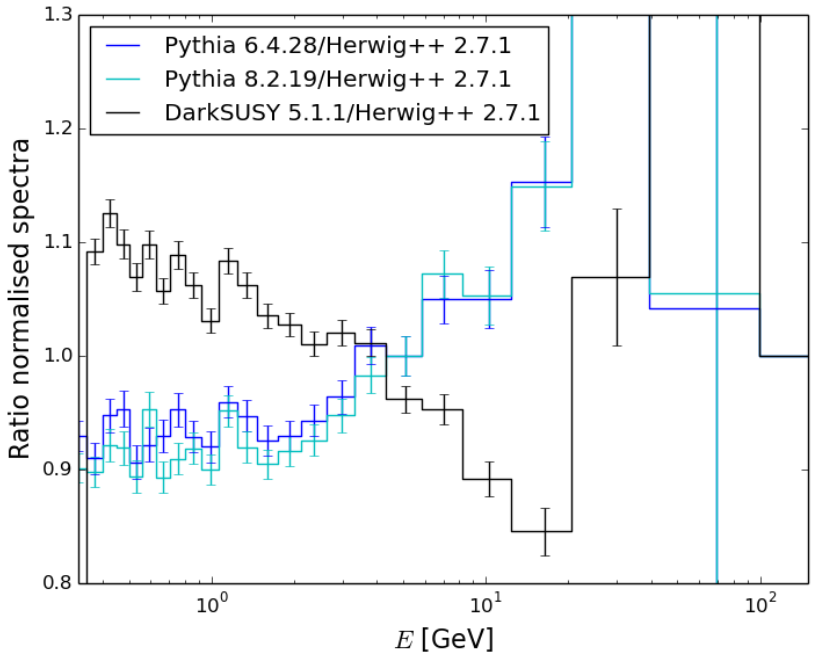

Figure 18: Ratio of the normalised spectra with the newer tunes, as well as a simulation in DarkSUSY 5.1.1.

for all relevant bins. At least the last 3 bins can not be taken into account for the same reason as mentioned in earlier sections. DarkSUSY indeed agrees most with HERWIG++.

The Standard Model simulations agree within an estimated error of 10%, while DarkSUSY only agrees with HERWIG++ within this estimate. Still, this conclusion can not be drawn with absolute certainty, as the error of the spectrum produced by DarkSUSY is unknown. If the uncertainty on the DarkSUSY spectrum is even slightly less then 10%, the spectrum agrees nearly completely with the PYTHIA spectra.

To investigate this further, a comparison with the Fermi/LAT data is performed in the next section.

4.5 Comparison with the Fermi/LAT data

In figure 19, the spectra of all the Standard Model simulations and `DarkSUSY` are plotted with the data. All spectra are normalised. It is important to state that the measurement also has an uncertainty in the energy, which is not taken into account here. So, it is possible that the real spectrum has a shifted peak or a tilted spectrum with respect to the spectrum shown in figure 19. But as this uncertainty is not taken into account here, the fits are actually better than pictured here. The `PYTHIA 8` spectrum plus additional error fit the data reasonably, so if a spectrum fits the data about as well as `PYTHIA 8`, it agrees with the data as well. As conclusions like these are difficult to

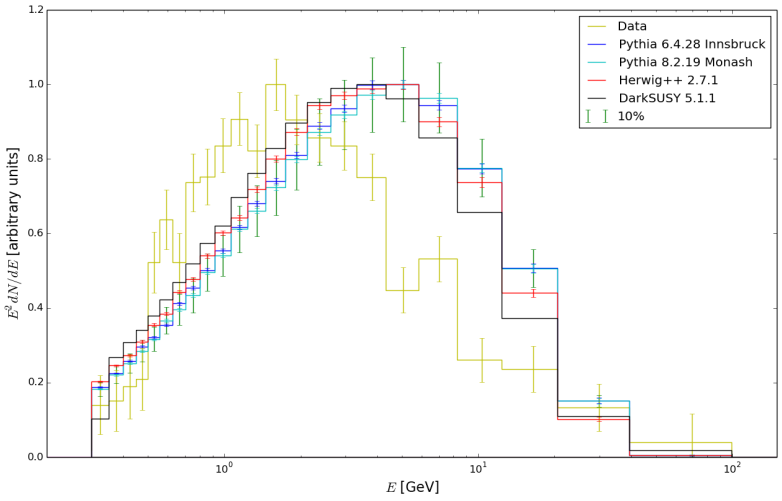

Figure 19: The normalised spectra performed with the newer tunes, including a simulation in `DarkSUSY 5.1.1` as well as the Fermi/LAT data.

draw from plots like figure 19, the ratios of all the spectra with the data are shown in figure 20.

As the uncertainty of the measured flux is so large, the ratios of all simulated spectra approximately lie within each others uncertainty bands. So they all agree with the data about equally well. The involved uncertainties are too large to see differences in how well the programmes fit. It is appropriate to draw the conclusion that all simulations fit the data relatively well, as `PYTHIA 8` fits the data and they all agree within the uncertainty of the ratios. Even if an additional error is needed for `DarkSUSY` to agree with `PYTHIA 8`, the uncertainty on the measurement is large enough to let their ratios with the data agree. The difference between the two is smaller than the error determined by the uncertainty of the measurement and the statistical error of the simulation of the spectrum in `PYTHIA 8`. This makes it practically impossible to draw a conclusion about which one fits the data better from figures 19 and 20 alone.

Furthermore, as the uncertainty is so large, it is not the best way to normalise by the peak height. It would have been better to normalise by an optimisation of the χ^2-value, while taking this reduction of the degrees of freedom into account in its calculation, but it is still good to show the Fermi/LAT spectrum at this point. This method involves minimising the overall difference between all spectra and the data, which helps with finding the optimal normalisation.

It is possible to draw the conclusion that the 10% error estimate from [11] is reasonable, as all Standard model simulations agree well with this estimate and the spectrum produced by `DarkSUSY` would, if an uncertainty of even less then 10% would be included. Also, the spectra fit the data equally well, which means that the p-value of 0.35 from [11] does not change significantly when

other simulations than PYTHIA 8 are also taken into account and also that the comparison with the Fermi/LAT data does not change the conclusion from section 4.4.

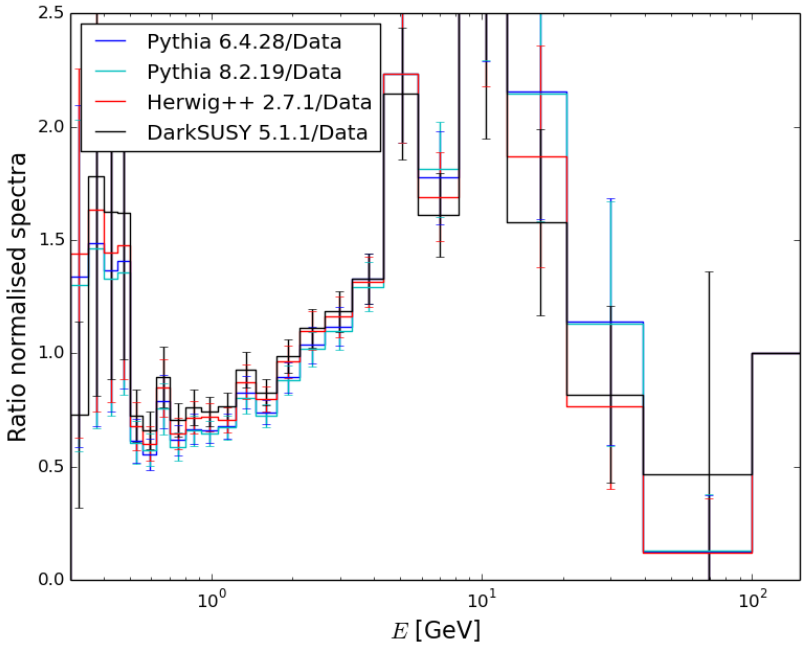

Figure 20: Ratio of the normalised spectra with the newer tunes, as well as a simulation in DarkSUSY 5.1.1 and the Fermi/LAT data.

4.6 Comparison of the Different Diagrams

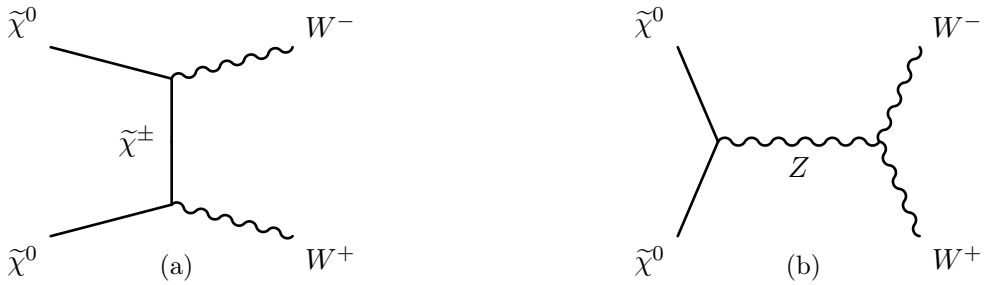

Figure 21: The dominant annihilation diagrams for the Wino/Higgsino component of the neutralino $\widetilde{\chi}^0$ into a pair of W bosons.

Figure 22: The two dominant annihilation diagrams for $\nu_e\overline{\nu_e} \to W^+W^-$.

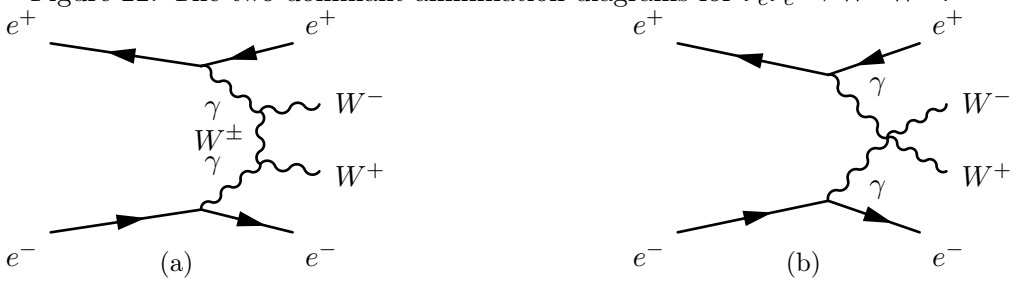

Figure 23: The two dominant annihilation diagrams for $e^+e^- \to \gamma\gamma \to W^+W^-$.

	$\widetilde{\chi}_0\widetilde{\chi}_0 \to W^+W^-$	$\nu_e\overline{\nu_e} \to W^+W^-$	$\gamma\gamma \to W^+W^-$
Energy incoming particle	$\sim$ 84.9 GeV	84.9 GeV	$\leq$ 84.9GeV
Spin incoming particle	half-integer	half-integer	integer
Mass intermediate particle (a)	$\mathcal{O}(100)$ GeV	0.5 MeV	80.39 GeV
Mass intermediate particle (b)	91.19 GeV	91.19 GeV	/
Mass incoming particle	84.9 GeV	$\sim$ 0	0

Table 1: A comparison of the diagrams pictured in figures 21, 22 and 23.

Figures 21, 22 and 23 again picture the dominant diagrams for neutralino annihilation into W^+W^-, The diagrams used to approach these in `PYTHIA 6` and 8 and the ones used in `HERWIG++`, respectively.

These diagrams are compared regarding their most important properties in table 1. Per construction, the energies of the incoming particles are at least very similar. The energies of the incoming photons are equal or less than the neutralino mass of 84.9 GeV, as shown in figure 8. This is not desirable as it creates an additional uncertainty on the produced photon spectrum, as mentioned before. However, this uncertainty has been minimised by forcing the incoming photons to each have at least 99% of the energy of the incoming electrons. So, this is a negligible disadvantage of using this process to estimate $\widetilde{\chi}^0\widetilde{\chi}^0 \to W^+W^-$. Another disadvantage is the integer spin of a photon compared to the half-integer spin of a neutrino. Yet, the mass of the intermediate particle in the diagrams (a) is better for estimating this process than the one in $\nu_e\overline{\nu_e} \to W^+W^-$. The mass of the intermediate $W^\pm$ boson in 23a is with 80.39 GeV much higher than the mass of the very light intermediate electron (0.5 MeV) in 22a. In both cases the masses of the incoming particles are nearly 0 compared to the relatively heavy neutralino. This is no problem, as long as the energy is correct.

The mass of the incoming particle in (b) is correct for the case of neutrinos, and the diagram shown in figure 23b does not have an intermediate particle. So, the diagrams are only really similar for an extremely off shell Z-boson, which is another disadvantage of this process, although this most likely is a lower order effect than the wrong mass of the internal particle in (a).

So the process using photons is better regarding the mass of the intermediate particles in (a) and the process using neutrinos is better regarding the spin of the incoming particles and the mass of the intermediate particles in (b).

In conclusion, it is good to use different processes with different advantages to estimate an unknown process like the neutralino annihilation, and as the additional uncertainty on the energy of the incoming photons is minimal, the simulation in `HERWIG++` is a equally reliable estimate of the process than the simulation in `PYTHIA 6` and `8`.

In further research, it might be more adequate to use the same process in all the simulations. As the matrix element for $\nu_e\overline{\nu_e} \to W^+W^-$ is not incorporated in `HERWIG++ 2.7.1` by default, it might also be appropriate to use $e^+e^- \to W^+W^-$ directly, without the intermediate photons. This would imply that the mass of the intermediate particle in (a) would be even less suitable, as the intermediate particle in this diagram is a neutrino rather than an electron, but that difference is relatively small compared to the chargino mass, so the effect is probably small.

This processes chosen here have the advantage of a possible comparison between two processes with suitable spin on one hand and a suitable mass of the intermediate particle in the higher order diagram (a) on the other. Even if the mass of the internal particle in (b) is worse than for neutrinos, this is still true, because this most likely is a lower order effect compared to the better mass in (a). However, the model uncertainties of the simulations are most likely much larger than these effects.

4.7 e^-, e^+, p^+ and p^- Spectra

Analysing the absolute counts of particles other than photons can also lead to interesting information about the simulation's agreement. If they do agree, it means that the processes used to estimate the annihilation of neutralinos are, at least, similar. This would be an indicator for them being suitable to estimate the diagrams pictured in figure 21.

Also, as the Alpha Magnetic Spectrometer (AMS) experiment in the International Space Station (ISS) measures the spectra of antimatter [19], it could be really useful to predict the spectra of particles as anti-protons or positrons which are expected for an annihilation of neutralinos. Here, the goal is the same as in the case of the photon spectrum. A complete spectrum inclusive the uncertainties of the simulations.

The electron and positron spectra obtained by `HERWIG++`, `PYTHIA 6` tuned with the 2013 Innsbruck tune and `PYTHIA 8` tuned with the 2013 Monash tune are shown in figures 24 and 25 in absolute counts. All of the spectra agree very well with their corresponding anti-particle variant. The initial state has no charge in all of the cases, so the spectra of particles like e^- and their corresponding anti-particles, e^+ in this case, are extremely similar.

The spectra of the different programmes also agree fairly well with each other. Especially important are the position and the height of the peak. The position is at the mass of the W-boson (80.39 GeV), and the height is determined by it's branching ratio into e^+ or e^-, which is very well known from experiments. So both the position of the peak and the number of particles around the peak position have to match for the different simulations, which they do. The absolute counts for

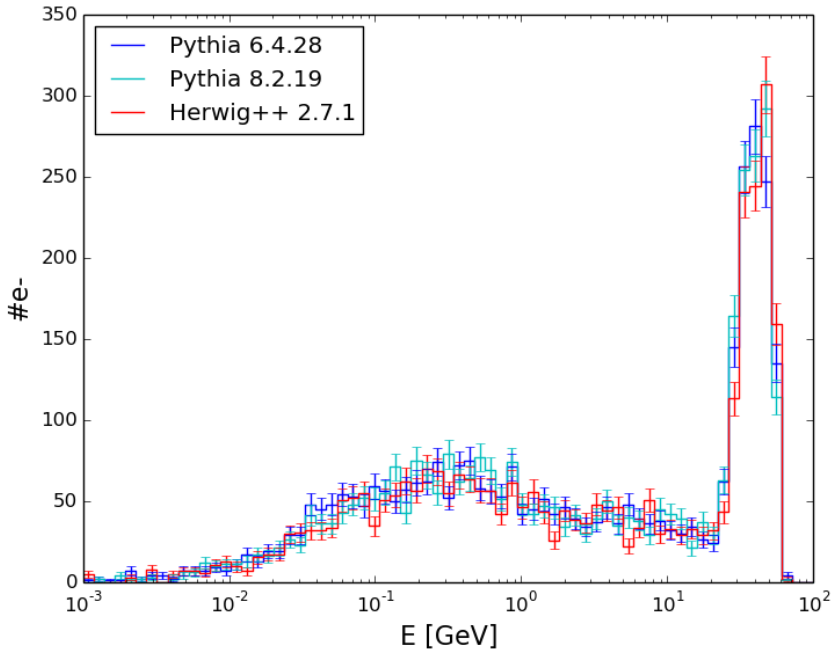

Figure 24: Absolute counts of e^- for the different simulations.

protons and anti-protons are shown in figures 26 and 27. In this case `HERWIG++` differs a little from both `PYTHIA 6` and `8`. However, this can be a product of the different hadronisation and fragmentation processes. Furthermore, the difference between the corresponding protons and anti-protons spectra of each simulation again agree very well. Which also indicates that the assumption that the

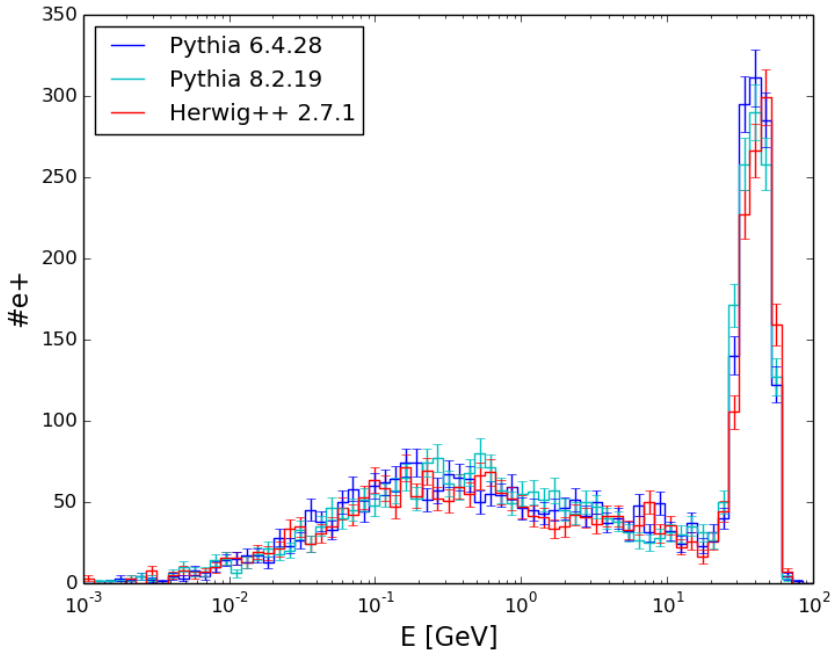

Figure 25: Absolute counts of e^+ for the different simulations.

difference of the PYTHIA spectra and the HERWIG++ spectrum is due to the different models.

This is a quite interesting finding and further investigation is needed to conclude where exactly the difference originates from.

All in all, these spectra agree with both the process used in HERWIG++ ($\gamma\gamma \to W^+W^-$) and the one used in PYTHIA ($\nu_e\overline{\nu_e} \to W^+W^-$) being adequate for approaching the neutralino annihilation into W-bosons.

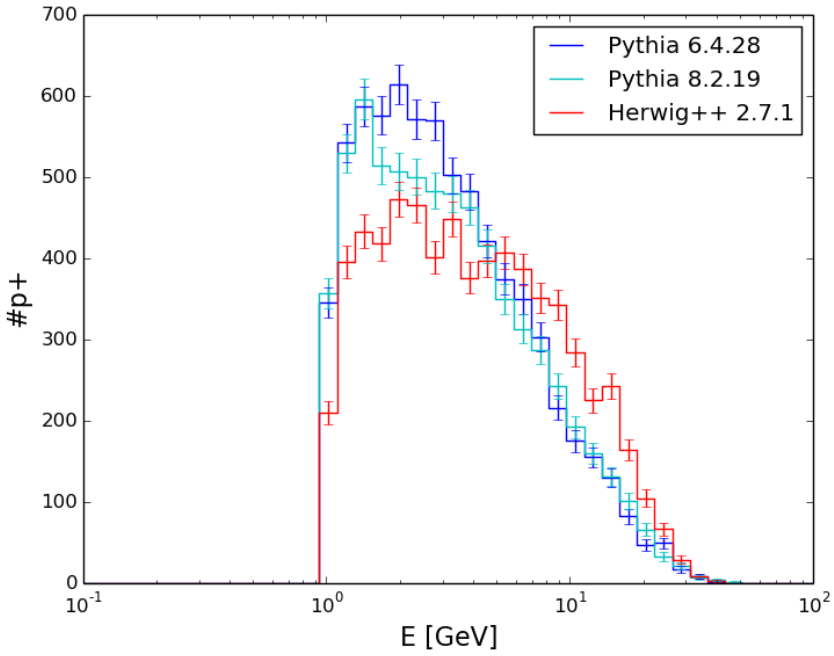

Figure 26: Absolute counts of protons for the different simulations.

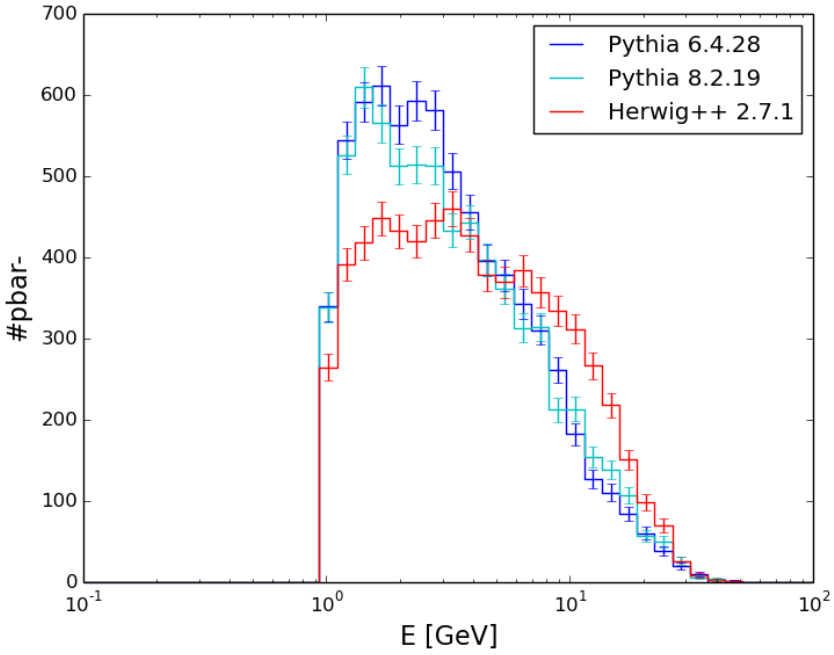

Figure 27: Absolute counts of anti-protons for the different simulations.

5 Conclusion & Outlook

We have compared spectra for the annihilation of neutralinos produced in HERWIG++ version 2.7.1 with PYTHIA 6.4.16 and PYTHIA 8.2.19 for standard tunes. The aim was to test wether an error of 10% on the spectrum produced by PYTHIA 8, which is needed for the spectrum to fit the data, is reasonably large (see section 4.2). This comparison seems to confirm the estimated error.

Switching to the 2013 Innsbruck tune [16] in PYTHIA 6.4.28 and the 2013 Monash tune [17] in PYTHIA 8.2.19, the spectra agree extremely well within this estimated error, which is another confirmation of this conclusion (see section 4.3). The conclusion was furthermore strengthened by a comparison with the flux as tabulated in DarkSUSY 5.1.1 (see section 4.4) and a comparison with the data from Fermi/LAT (see section 4.5).

All in all, the conclusion can be drawn that the estimated 10% error on the simulation in PYTHIA 8 is indeed reasonable. So, it can be concluded that the galactic centre solution described in [11] is valid.

Also, it is possible to perform an automated variation of the shower parameters like the parameters of the fragmentation function in PYTHIA 8 [20]. This only estimates the theoretical uncertainty of the simulation and does not estimate the error made by approaching a dark matter particle by a standard model particle. Even though this error is completely unknown, it is estimated to be very small.

So, an estimate of the theoretical error by an automated shower variation is probably a very good estimate of the uncertainty of the photon spectrum and from a comparison with the spectra produced in HERWIG++ and PYTHIA 6, one can conclude a complete simulated gamma spectrum plus uncertainty bands. For this, a tuning or a shower variation for both HERWIG++ and PYTHIA 6 can be very useful, because in that case one could essentially compare three spectra plus uncertainty bands with each other instead of just the spectra. It is not particularly important if the same processes are used in all of the simulations, as the effect of the different models of the simulations themselves are most likely much of much more importance.

The difference between HERWIG++ and both versions of PYTHIA in the case of both the proton and the anti-proton spectra is also something which needs further investigation. A complete spectrum inclusive an (automated) shower variation would be just as interesting in this case. It would be especially interesting to know wether the difference between HERWIG++ and both versions of PYTHIA can be explained by this variation. If it can not, there has to be further investigation to find the reason for the difference.

So in conclusion, a shower variation for PYTHIA 6 and HERWIG++, as well as an automated shower variation for PYTHIA 8, might be the key to fully check if all the spectra produced by different simulations are in complete agreement with each other and, if they are not, where exactly they deviate and why. This is an extremely important step towards a detailed simulation of spectra expected from a neutralino annihilation inclusive uncertainty bands.

References

[1] V. C. Rubin, W. K. Ford, Jr., and N. Thonnard, *Rotational properties of 21 SC galaxies with a large range of luminosities and radii, from NGC 4605 R = 4kpc to UGC 2885 R = 122 kpc*, *Astrophysical Journal* **238** (June, 2000) 471–487.

[2] Y. Sofue and V. Rubin, *Rotation Curves of Spiral Galaxies*, astro-ph/0010594.

[3] D. Clowe, M. Bradač, A. H. Gonzalez, M. Markevitch, S. W. Randall, C. Jones, and D. Zaritsky, *A direct empirical proof of the existence of Dark Matter*, astro-ph/0608407.

[4] Planck Collaboration, *Planck 2015 results. XIII. Cosmological parameters*, arXiv:1502.01589.

[5] V. Vitale, A. Morselli, and Fermi/LAT Collaboration, *Indirect Search for Dark Matter from the center of the Milky Way with the Fermi-Large Area Telescope*, arXiv:0912.3828.

[6] F. Calore, I. Cholis, and C. Weniger, *Background model systematics for the Fermi GeV excess*, arXiv:1409.0042.

[7] J. F. Navarro, C. S. Frenk, and S. D. White, *A Universal Density Profile from Hierarchical Clustering*, *Astrophysical Journal* **490** (Octobre, 1997) 493–508, [astro-ph/9611107].

[8] T. Daylan, D. P. Finkbeiner, D. Hooper, T. Linden, S. K. N. Portillo, N. L. Rodd, and T. R. Slatyer, *The Characterization of the Gamma-Ray Signal from the Central Milky Way: A Compelling Case for Annihilating Dark Matter*, arXiv:1402.6703.

[9] I. Cholis, D. Hooper, and T. Linden, *Challenges in Explaining the Galactic Center Gamma-Ray Excess with Millisecond Pulsars*, arXiv:1407.5625.

[10] R. M. O'Leary, M. D. Kistler, M. Kerr, and J. Dexter, *Young and Millisecond Pulsar GeV Gamma-ray Fluxes from the Galactic Center and Beyond*, arXiv:1601.05797.

[11] A. Achterberg, S. Amoroso, S. Caron, L. Hendriks, R. R. de Austri, and C. Weniger, *A description of the Galactic Center excess in the Minimal Supersymmetric Standard Model*, arXiv:1502.05703.

[12] T. Bringmann and C. Weniger, *Gamma Ray Signals from Dark Matter: Concepts, Status and Prospects*, arXiv:1208.5481.

[13] T. Sjöstrand, S. Mrenna, and P. Skands, *Pythia 6.4 - Physics and Manual*, hep-ph/0603175.

[14] M. Bähr, S. Gieseke, M. Gigg, D. Grellscheid, K. Hamilton, O. Latunde-Dada, S. Plätzer, P. Richardson, M. Seymour, A. Sherstnev, J. Tully, and B. Webber, *Herwig++ Physics and Manual*, arXiv:0803.0883.

[15] J. A. R. Cembranosa, A. de la Cruz-Dombriz, V. Gammaldia, R. A. Linerosd, and A. L. Marotoa, *Reliability of Monte Carlo event generators for gamma-ray dark matter searches*, arXiv:1305.2124.

[16] N. Firdous and G. Rudolph, *Tuning of PYTHIA6 to Minimum Bias Data*, *EPJ Web of Conferences* **60** (November, 2013).

[17] P. Skands, S. Carrazza, and J. Rojo, *Tuning PYTHIA 8.1: the Monash 2013 Tune*, arXiv:1404.5630.

[18] P. Gondolo, J. Edsjo, P. Ullio, L. Bergstrom, M. Schelke, and E. Baltz, *DarkSUSY: Computing Supersymmetric Dark Matter Properties Numerically*, *JCAP* **0407** (June, 2004) 008, [astro-ph/0406204].

[19] M. Aguilar et al. (AMS Collaboration), *First Result from the Alpha Magnetic Spectrometer on the International Space Station: Precision Measurement of the Positron Fraction in Primary Cosmic Rays of 0.5 - 350 GeV*, *Phys. Rev. Lett.* **110** (April, 2013) 141102.

[20] S. Mrenna and P. Skands, *Automated Parton-Shower Variations in Pythia 8*, arXiv:1605.08352.